Electronic Supplementary Material (ESI) for Nanoscale.

Electronic Supplementary Information

Binding of Tyrosine Kinase Inhibitor to epidermal growth factor receptor: Surface-Enhanced Infrared Absorption Microscopy reveals subtle secondary structure variations

Paolo Zucchiatti, [a,b] Giovanni Birarda, [a] Andrea Cerea, [c] Marta S. Semrau, [a] Aliaksandr Hubarevich, [c] Paola Storici, [a] Francesco De Angelis, [c] Andrea Toma [c] and Lisa Vaccari [a]*

*Email address: lisa.vaccari@elettra.eu

Table of Contents

Estimation of the Enhancement Factor (EF)

The enhancement factor induced by the nanoantenna array was evaluated by comparing SEIRA spectra with a reference signal acquired through conventional FTIR spectroscopy. Figure S1a summarizes these measurements, illustrating spectral results recorded on BSA film of comparable thickness, $t \approx 7$ nm, as measured by Atomic Force Microscopy (AFM). In both cases, the illumination area has been fixed to 40 x 40 μm^2, and average spectra of 6 measurements on different matrices have been reported.

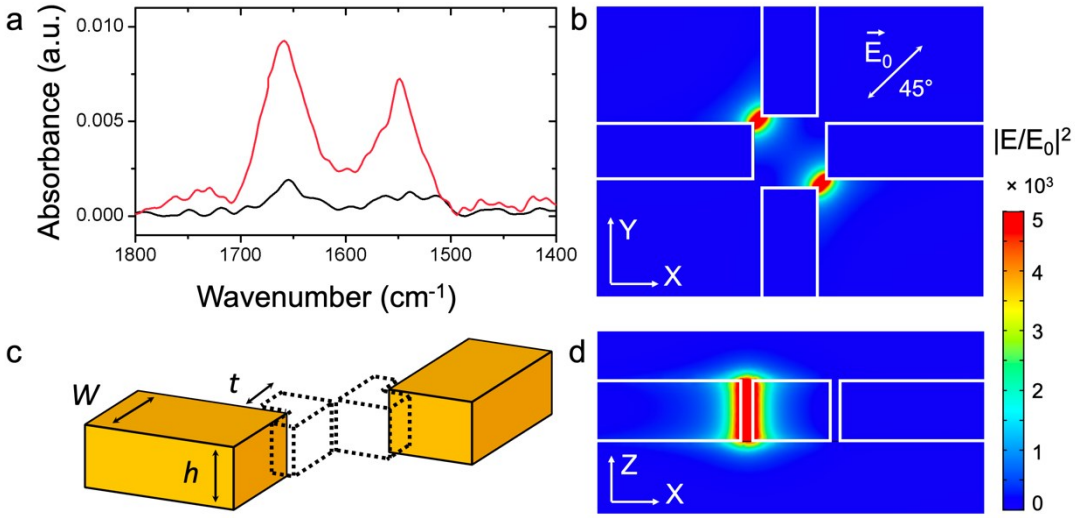

Figure S1: (a) Comparison between SEIRA extracted spectrum (red line) and conventional FTIR absorbance signal (black line) acquired on a BSA film of comparable thickness. (c) Schematic view of the nanogap region enclosed between two adjacent nanoantennas, the dashed lines indicate the active volume used for the EF evaluation. (b, d) Two-dimensional maps (top and lateral views, respectively) of the field enhancement around the gap region at the nanoantenna resonant wavelength (λ = 6.04 μm).The local electric field $\vec{E}$ has been normalized to the incoming electric field $\vec{E}_0$, while the polarization direction has been indicated by a white arrow.

By comparing the vibrational peak associated to Amide I band (ω_{vib} = 1654 cm^{-1}) we can immediately appreciate a remarkable increase in the signal intensity, of about a factor of 5. This result is of particular

significance since most of the signal enhancement occurs in the nanogap region, covering an area markedly smaller than the overall sensing surface.

Within this context and to precisely evaluate the EF of the nanoantenna array, the different volumes contributing to the SEIRA and reference signals were taken into account. For this reason, the spatial distribution of the enhanced field was evaluated recurring to COMSOL Multiphysics (RF module, Finite Element Method). As highlighted in Figure S1b and d, the nanoantennas convert the impinging Electromagnetic radiation into an extremely localized optical field, which intensity is significantly enhanced within the nanogap region. The spatial extension of these hot-spots can be assumed to approximately coincide with the "nano-boxes" depicted in Figure S1c, *i.e.*, $4 \times t \times h \times (t + W/2) \cong 1.3 \times 10^5$ nm^3. Molecules adsorbed on these sites dominate the total SEIRA signal, therefore in accordance to [1,2] , we used this volume to calculate the EF. Since the ratio between the active region in SEIRA and conventional FTIR measurements is ~ 1:250, an EF $\cong 10^3$ has been retrieved.

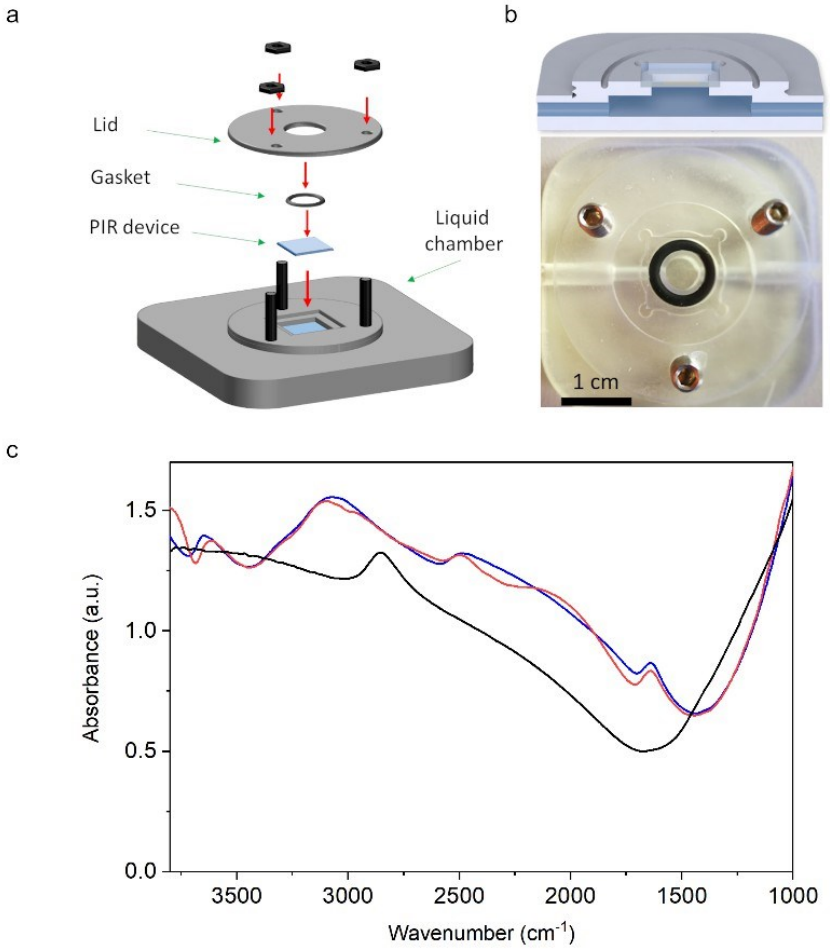

Figure S2: (a) Exploded view of the fluidic device for PIR-SEIRA measurements made by 3D printing. (b) Top view of the fluidic device: the inlet and outlet channels are visible through the transparent plastic. The device cross-section sketch, where channel housings are visible, is also shown. (c) PIR-SEIRA spectra of water (blue line) and HEPES buffer (red line) compared with the bare-device SEIRA response in dried conditions (black line).

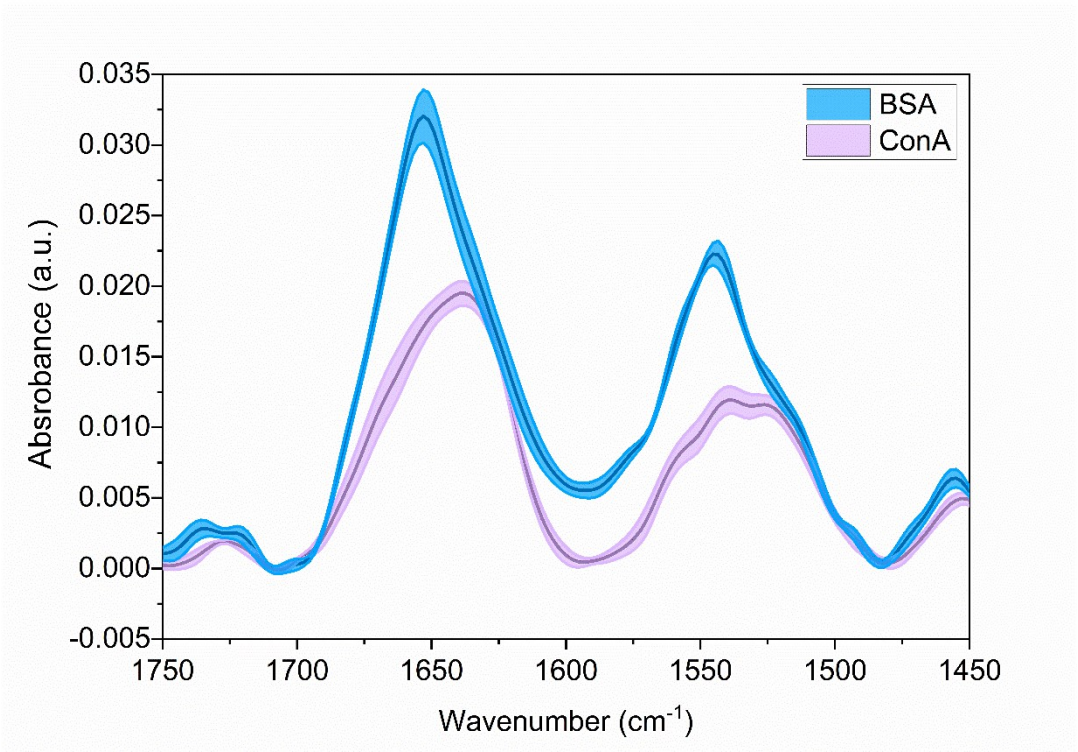

Figure S3: PIR-SEIRA average absorbance spectra ± standard deviation of BSA (black continuous line ± light violet profile) and ConA (black continuous line ± light blue profile), anchored onto the plasmonic devices by amine coupling protocol. Spectral profile thickness corresponds to the standard deviations of n=10 measurements.

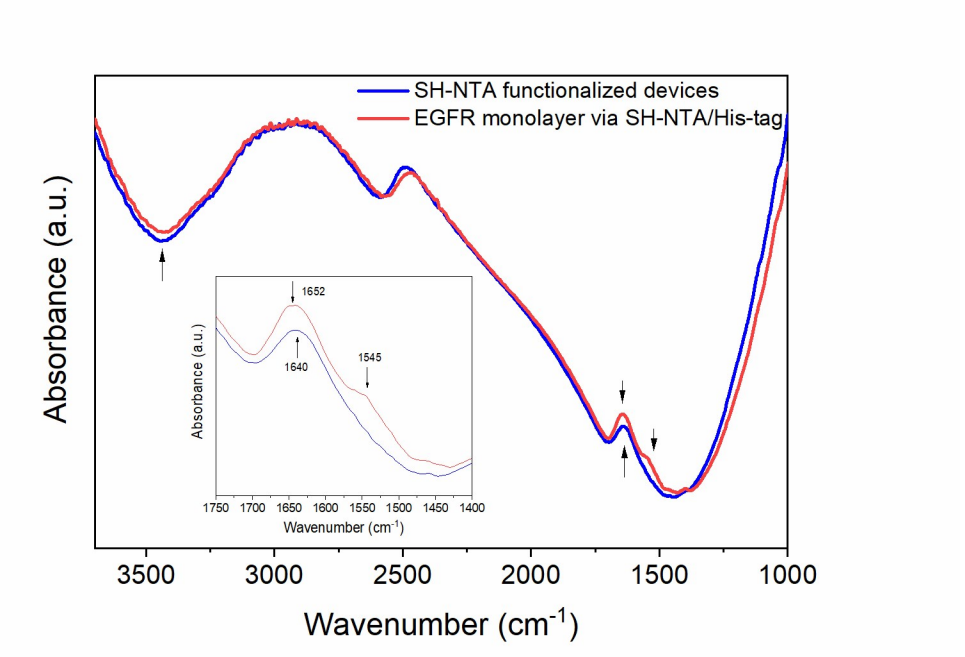

Figure S4: PIR-SEIRA measurements on SH-NTA functionalized antennas (blue spectra) and antennas functionalized with *wt* EGFR_KD via SH-NTA/His-tag methodology (red spectra). Vertical downward arrows highlight protein Amide bands, while upward arrows highlight aqueous contributions. In the inset, a zoom of the Amide I-Amide II region is plotted. The arrows point to the water bending mode for SH-NTA functionalized antennas, and Amide I and Amide II bands for *wt* EGFR_KD.

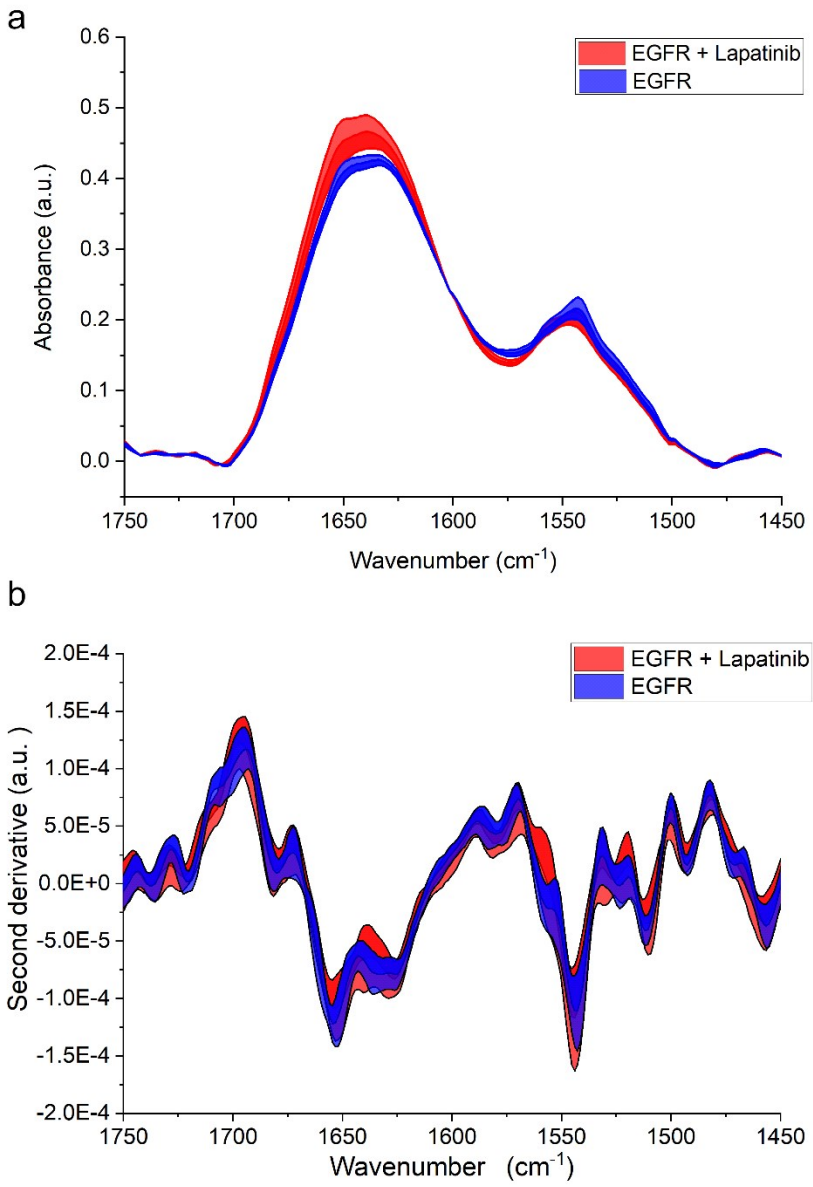

Figure S5: (a) Average absorbance spectra of *wt* EGFR_KD (blue spectrum) and Lapatinib-EGFR_KD. The spectral thickness corresponds to the standard deviation of n=10 measurements. (b) Average second derivative of *wt* EGFR_KD (blue spectrum) and Lapatinib-EGFR_KD. The spectral thickness corresponds to the standard deviation of n=10 measurements.

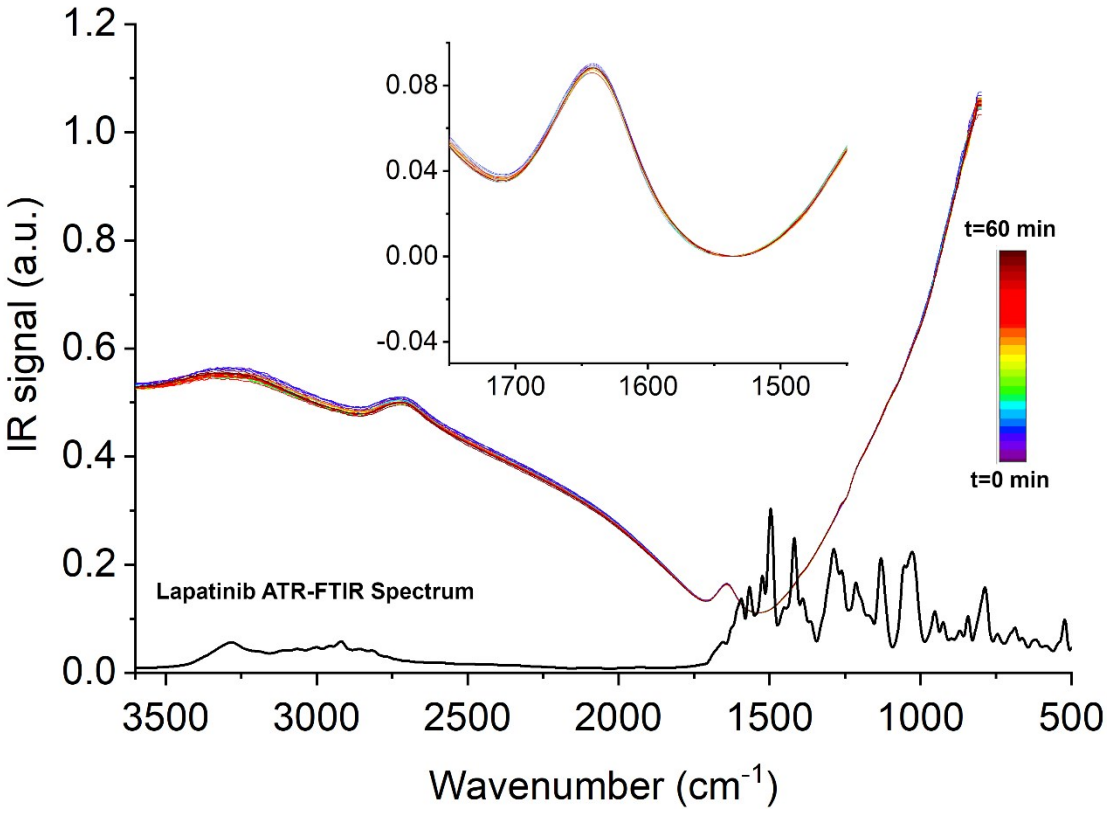

Figure S6: Black line: ATR-FTIR spectrum of Lapatinib, obtained letting dry Lapatinib (lapatinib ditosylate hydrate, C29H26ClFN4O4S • 2 (C7H8O3S) • H2O) solution 30mM in DMSO onto the diamond Internal Reflection Element (IRE) of the single-reflection PLATINUM ATR accessory (Bruker GmbH). The spectrum has been collected averaging 256 scans at 4 cm^{-1} spectral resolution. The Lapatinib most intense spectral features in the 1750-1450 cm^{-1} spectral region are peaked at 1500, 1524, 1567 and 1594 cm^{-1}. A broad and much less intense band is peaked at 1656 cm^{-1}. Rainbow colored series: Lapatinib solution 300nM was flushed within a pristine PIR device (without protein anchored) and PIR spectra were acquired for 60 minutes. Inset: zoom in the 1750-1450 cm^{-1} spectral region, showing that there are no detectable spectral variations in the considered spectral range, proving that the non-specific anchoring of Lapatinib is non-detectable even on bare nanoantennas.

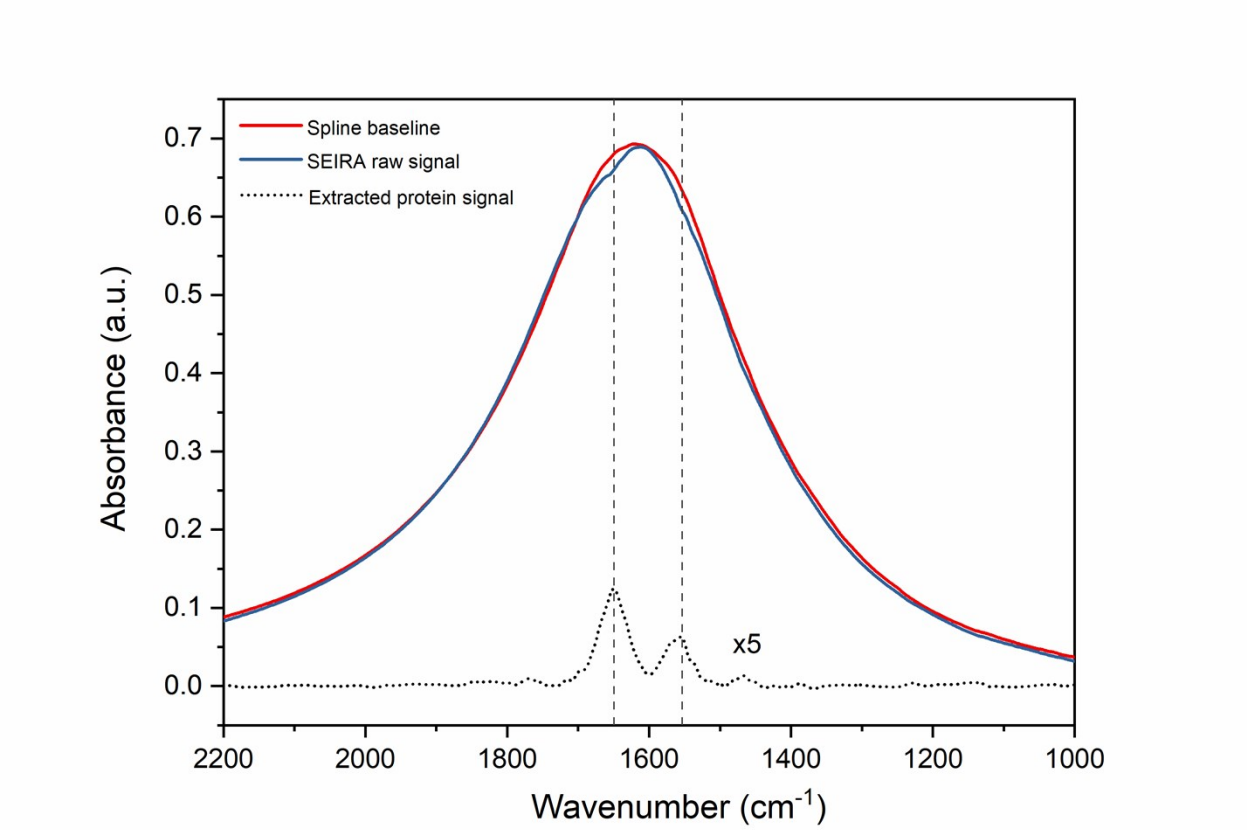

Figure S7: Extraction of protein signals: SEIRA resonance raw signal of functionalized devices (continuous navy line) was baseline corrected by fitting a polynomial spline curve (continuous red line).[3] The extracted spectrum, obtained by subtracting the fitted baseline from the resonance raw signal and reversing the resulting spectrum, shows the enhanced Amide I and II spectral bands.

REFERENCES

1 C. D'Andrea, J. Bochterle, A. Toma, C. Huck, F. Neubrech, E. Messina, B. Fazio, O. M. Maragò, E. Di Fabrizio, M. Lamy de La Chapelle, P. G. Gucciardi and A. Pucci, *ACS Nano*, 2013, **7**, 3522–3531.

2 J. Li, Z. Yan, J. Li, Z. Wang, W. Morrison and X.-H. Xia, *Nanoscale*, 2019, **11**, 18543–18549.

3 I. J. Schoenberg, in *On Approximation Theory / Über Approximationstheorie: Proceedings of the Conference held in the Mathematical Research Institute at Oberwolfach, Black Forest, August 4–10, 1963 / Abhandlungen zur Tagung im Mathematischen Forschungsinstitut Oberwolfach, Schwarzwald, vom 4.–10. August 1963*, eds. P. L. Butzer and J. Korevaar, Springer, Basel, 1964, pp. 109–129.